Research Paper
Journal of Aerospace System Engineering
Vol.15, No.2, pp.1-9 (2021)
EISSN 2508-7150
http://dx.doi.org/10.20910/JASE.2021.15.2.1

Structural Optimization of a Thick-Walled Composite Multi-Cell Wing Box Using an Approximation Method

San-Hui Kim[1,†], Pyung-Hwa Kim[1], Myung-Jun Kim[2] and Jung-sun Park[3,†]
[1]Graduate School of Aerospace and Mechanical Engineering, Korea Aerospace University
[2]Department of Aviation Maintenance Engineering, Silla University
[3]Department of Aerospace and Mechanical Engineering, Korea Aerospace University

Abstract

In this paper, a thickness compensation function is introduced to consider the shear deformation and warping effect resulting from increased thickness in the composite multi-cell wing box. The thickness compensation function is used to perform the structure optimization of the multi-cell. It is determined by minimizing the error of an analytical formula using solid mechanics and the Ritz method. It is used to define a structural performance prediction expression due to the increase in thickness. The parameter is defined by the number of spars and analyzed by the critical buckling load and the limited failure index as a response. Constraints in structural optimization are composed of displacements, torsional angles, the critical buckling load, and the failure index. The objective function is the mass, and its optimization is performed using a genetic algorithm.

Key Words: Wing Box, Multi-Cell, Thick-Walled Structure, Structural Optimization, Ritz Method

1. Introduction

Aerospace structures used in the aerospace industry require optimization for high performance and low cost, and studies pertaining to it have been actively carried out. Various methods are used to approximate the structural performance of composite structures. For efficient structural analysis, the structural performance prediction technique is defined using the Ritz method, which is an approximation method. Furthermore, it is necessary to increase the thickness of the wing box consisting of skin, spars, and ribs as a way of improving the effective stiffness of aircraft wings. Here, the shear deformation and warping effect caused by the increase in thickness should be considered.

Therefore, based on the theoretical analysis considering the shear deformation and warping effect, we have defined the compensation function according to the thickness increase and applied it to the structural performance prediction method. Through this, it is possible to predict the structural performance of a wing box having a thick thickness subject to shear deformation or warping effect.

For the structural optimization of a composite multi-cell wing box, the wing box is assumed to have a thin-walled composite beam structure, and the contour parameters of the thin-walled beam structure can be used to find the effective stiffness. By applying the compensation function for thickness, the contour parameters that can be applied to a thin-walled structure are applied to a thick-walled structure to perform the structure optimization of the wing box to improve the efficiency and accuracy in repetitive analysis.

2. Discussion

2.1 Definition of Stiffness Using Contour Parameters

Several methods can be used for calculating the stiffness of typical structures, but the contour parameters are used to calculate the effective stiffness of a thin-walled composite structure [1]. The contour coordinates and contour line are generated along the surface of the structure, and “s” which represents a contour parameter is defined on the coordinate system.

Received: Apr. 29, 2020 Revised: Aug. 12, 2020 Accepted: Aug. 14, 2020
† Corresponding Author
Tel: +82-02-300-0114, E-mail: jungsun@kau.ac.kr
Ⓒ The Society for Aerospace System Engineering

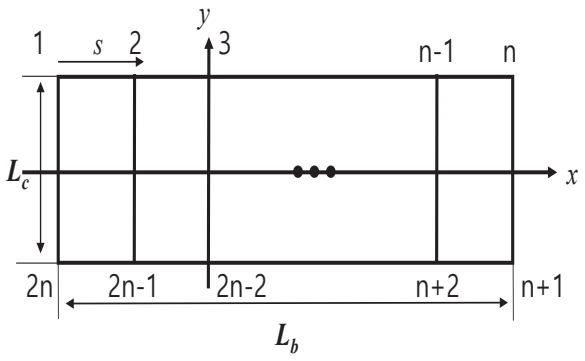

Fig. 1 Cross-section shape of multi-cell wing box

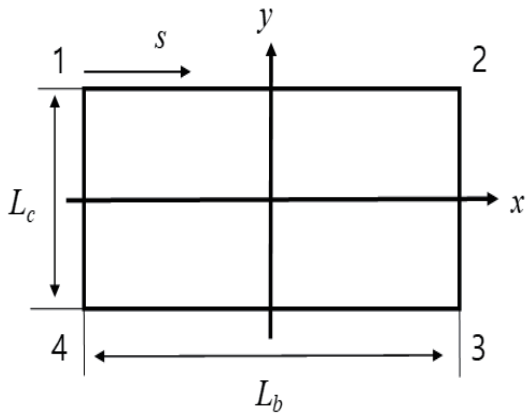

Fig. 2 Cross-section shape of single-cell wing box

The cross-section shape of the multi-cell wing box for setting the contour parameters is shown in Fig. 1. Fig. 2 shows the contour parameters for a single cell, which is a portion taken from the multi-cell. That is, Fig. 2 shows the cross-section of a single cell, which is a part of the multi-cell. If the contour parameter is applied, Eqs. (1), (2), (3), and (4) are derived [2].

$$1-2: s=x,\ x_e=x,\ y_e=\frac{L_c}{2} \tag{1}$$

$$2-3: s=\left(\frac{L_c}{2}-y\right),\ x_e=\frac{L_b}{2},\ y_e=-y \tag{2}$$

$$3-4: s=\left(\frac{L_b}{2}-x\right),\ x_e=-x,\ y_e=-\frac{L_c}{2} \tag{3}$$

$$4-1: s=\left(\frac{L_c}{2}+y\right),\ x_e=-\frac{L_b}{2},\ y_e=y \tag{4}$$

Eqs. (5), (6), (7), (8), (9), and (10) are equations that find S (axial stiffness) and D (bending stiffness) using the contour parameters.

$$S=\int_s D\,ds \tag{5}$$

$$S_x=\int_s D y_e\,ds \tag{6}$$

$$S_y=\int_s D x_e\,ds \tag{7}$$

$$D_x=\int_s D y_e^2\,ds \tag{8}$$

$$D_y=\int_s D x_e^2\,ds \tag{9}$$

$$D_{xy}=\int_s D x_e y_e\,ds \tag{10}$$

The bending stiffness of the multi-cell is defined through this. If the torsional stiffness is defined using a similar method, it can be expressed as Eq. (11).

$$D_{torsion}=\frac{1}{4A^2}\int\frac{ds}{A_{66}} \tag{11}$$

Where A denotes the width of the cross-section. Through these, the bending stiffness and the torsional stiffness can be obtained, respectively.

The bending angle and twist angle were obtained to verify the effective stiffness of the thin-walled composite multi-cell wing box. They were compared to the experimental data on a thin-walled beam like the one shown in Fig. 2 to verify the calculation process [3]. The model was set to a box-shaped beam with the cross-section of Fig. 1, and the bending analysis results and the torsional analysis results are shown in Figs. 3 and 4, respectively. The comparison result shows that the error is not large, and based on this, it is confirmed that the definition of stiffness for bending and torsion of the thin-walled wing box is valid.

$$w(x)=\sum_{i=1}^{5}a_i x^{i+1}(x^3-2x^2L_a+2{L_a}^3) \tag{13}$$

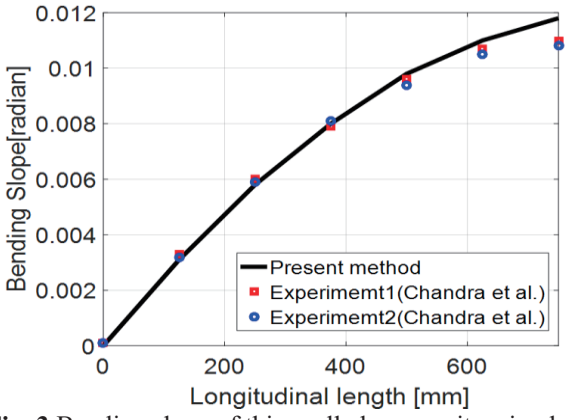

Fig. 3 Bending slope of thin-walled composite wing box

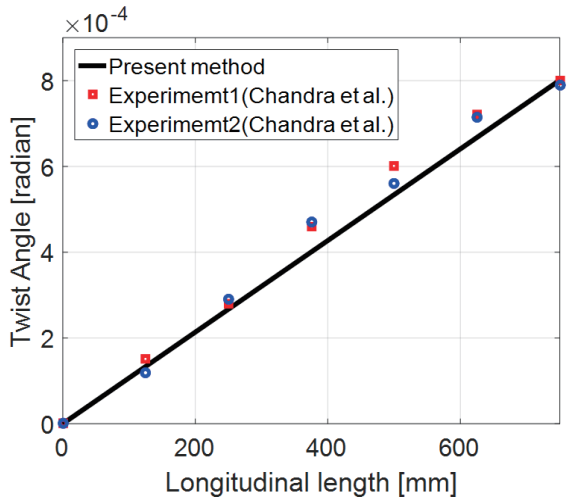

Fig. 4 Torsional angle of thin-walled composite wing box

2.2 Structural Performance Prediction Method

2.2.1 Bending Analysis and Prediction Method of Composite Wing Box

The structural performance prediction method was defined for the bending analysis of a composite multi-cell wing box. The bending stiffness defined above was applied, and the Ritz vector considering the boundary condition was set up to use the Ritz method [4].

The Ritz vector was set using Eq. (13), which is w (z-direction displacement) that satisfies the end-fixed support boundary condition, Eq. (12), and the load condition is the height-direction load of the free edge, as shown in Fig. 5.

$$w(0) = \frac{\partial w(0)}{\partial x} = 0 \tag{12}$$

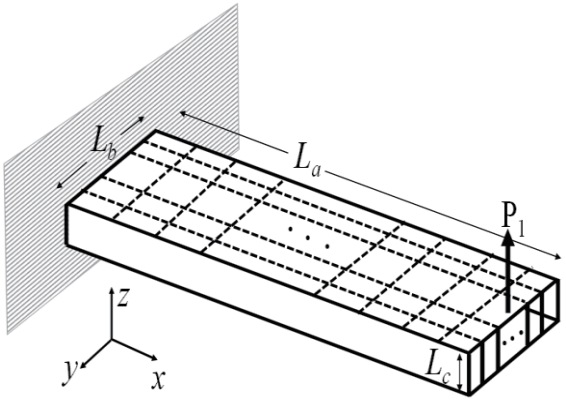

Fig. 5 Bending analysis model of composite wing box

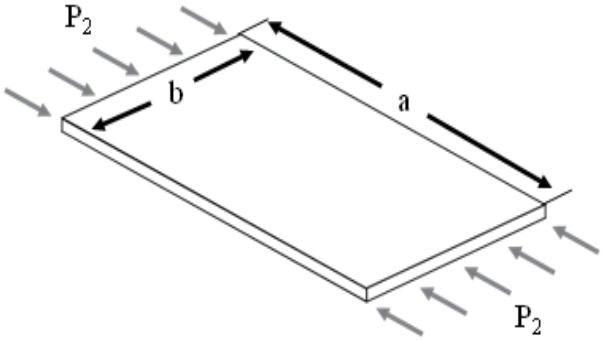

Fig. 6 Buckling analysis model of composite wing box skin

To use the Ritz method, it is necessary to calculate the work by the deformation energy and external force by using a contour function.

$$U = \frac{1}{2}\int \{D_{bending}\left(\frac{\partial^2 w}{\partial^2 x}\right)^2\} \tag{14}$$

$$W = w(L_a) \times P \tag{15}$$

When the variation of the Ritz vector for the sum of deformation energy and external work becomes 0 according to the minimum total energy principle, it has the minimum total energy, which can be expressed as Eq. (16):

$$\frac{\partial}{\partial a_i}(U - W) = 0 \tag{16}$$

By finding the solution for the linear matrix problem in Eq. (16), the Ritz vector value can be calculated. Through the Ritz vector value obtained as a calculation result, the deflection equation for the z-direction displacement can be derived.

2.2.2 Buckling Analysis and Prediction Method of Composite Wing Box

The buckling analysis and prediction method of a composite multi-cell wing box was defined. To use the Ritz method, it is necessary to set a Ritz vector that satisfies the boundary condition [5]. The contour function was set as w (z-direction displacement) of Eq. (17) that satisfies the simple support of four-sides, and the load condition is the longitudinal compressive load at the end, as shown in Fig. 6. The buckling analysis and prediction method assume that local buckling on the skin occurs. Because reinforcement can be applied to the wing box, it is safe to proceed with the analysis focusing on the local buckling of the skin [6].

$$w(x,y) = \sum_{I=1}^{M}\sum_{J=1}^{N} Z_{IJ}F_I(x)G_J(y) \tag{17}$$

If the deformation energy and the work done by the external force are calculated in the form of the contour function, Eqs. (18), (19), and (20) can represent.

$$U = \frac{1}{2}\iint \{D(x,y)\}dA \tag{18}$$

$$D(x,y) = \begin{Bmatrix} D_{11}\left(\frac{\partial^2 w}{\partial x^2}\right)^2 + D_{22}\left(\frac{\partial^2 w}{\partial y^2}\right)^2 \\ +4D_{66}\left(\frac{\partial^2 w}{\partial x\,\partial y}\right)^2 \\ +2D_{12}\left(\frac{\partial^2 w}{\partial x^2}\right)\left(\frac{\partial^2 w}{\partial y^2}\right) \\ +4D_{16}\left(\frac{\partial^2 w}{\partial x^2}\right)\left(\frac{\partial^2 w}{\partial x\,\partial y}\right) \\ +4D_{26}\left(\frac{\partial^2 w}{\partial y^2}\right)\left(\frac{\partial^2 w}{\partial x\,\partial y}\right) \end{Bmatrix} \tag{19}$$

$$W = \frac{1}{2}P_x\iint \left(\frac{\partial w}{\partial x}\right)^2 dA \tag{20}$$

When the variation of the Ritz vector for the sum of the deformation energy and the external work becomes 0 according to the minimum total energy principle, it has the minimum total energy, which is expressed as Eq. (21):

$$\frac{\partial}{\partial Z_{IJ}}(U - W) = 0 \tag{21}$$

The eigenvalue problem is defined by Eqs. 22 and 23 to solve the buckling problem, and the critical buckling load and the contour mode can be derived through the eigenvalue and eigenvector.

$$[S][C] = P_{cr}[R][C] \tag{22}$$

$$[C] = [Z_{11} \cdots Z_{IJ}]^T \tag{23}$$

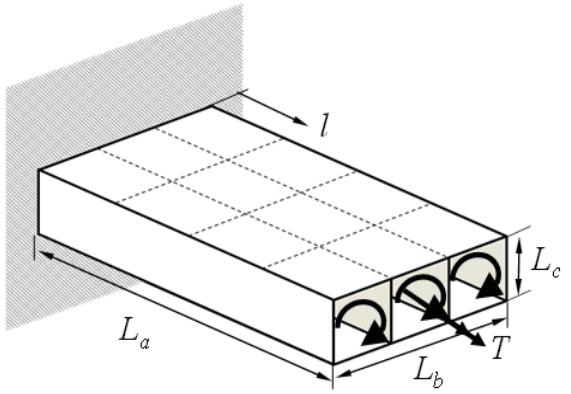

Fig. 7 Torsional analysis model of composite wing box

2.2.3 Torsional Analysis and Prediction Method of Composite Wing Box

For the twist angle of the wing box, the superposition method can be applied to each cell, and the twist angle is obtained using the torsional stiffness defined above. Eq. (24) is an analytical equation for the torsion of the composite multi-cell wing box shown in Fig. 7.

$$\theta_z = \frac{TL}{D_t} \tag{24}$$

2.3 Definition of Compensation Function Considering the Increase of Thickness

If the contour parameters are used, a wing box of a thin-walled beam structure shape can be analyzed conveniently. However, the calculation process and analysis is complex for a wing box of a thick-walled beam structure shape because the analysis must consider the shear deformation and the warping effect. Therefore, for convenient calculation, the analysis can be performed by efficiently reflecting the thickness effect through a verified compensation function. A mechanical theory equation was calculated to define the compensation function [7]. Several assumptions are required on the bases of thick-walled beam theory.

First, the in-plane deformation of the cross-section of the beam is not considered. Second, the horizontal shear effect of the beam is considered, and the shear deformation rate is assumed to change to a parabola. Third, the primary and secondary warping effects are considered.

Based on the above assumptions, the application criteria are set to $t_{max} \geq 0.1 \times L_b$ to assume that a thin beam is a thick-walled cell structure where t_{max} indicates the maximum thickness of the thick wall. Figs. 8 and 9 show the error between the bending and torsion analysis results and the theoretical equations, respectively. This error is the error between the theoretical equation and the defined analytical formula, and we performed regression analysis using a polynomial function to find a function that minimizes the error.

$$C_{bending} = f(\mu) = a\mu^2 + b\mu \tag{25}$$

$$C_{torsion} = g(\mu) = c\mu^2 + d\mu \tag{26}$$

where μ denotes the value obtained by dividing the maximum thickness t_{max} by L_b. Eqs. (25) and (26) are the compensation functions according to the thickness, and the coefficients are $a = 291.5, b = 48.6, c = 270.1, d = 99.91$.

2.4 Validation Using Finite Element Method Results

To verify the validity of the structural performance prediction method defined in this paper, the results were compared with the finite element analysis (FEA) results. The properties of T-700 composite were used, and the laminated pattern and the thickness of the composite are shown in Table 2. By setting cases 1, 2, 3, and 4, we compared the results between the structural performance prediction method and the finite element method (FEM) for each case when the thickness was increased to 2 mm, 6 mm, 10 mm, and 14 mm. For the load conditions, the bending load and the torsional moment at the end part were set to 4.45 kN and 113 kN · mm, respectively.

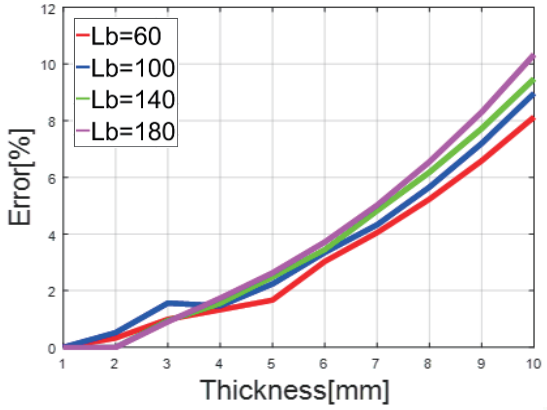

Fig. 8 Bending analysis result of error according to L_b

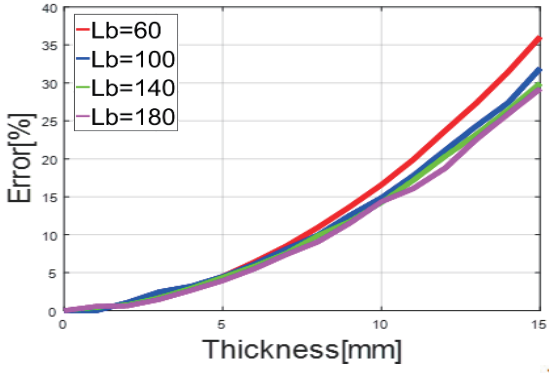

Fig. 9 Torsion analysis result of error according to L_b

Table 1 Parameters of the wing box

Parameters	Layups
L_a, Length(mm)	500
L_b, Length(mm)	50
L_c, Length(mm)	25
Layer thickness(mm)	0.125

Table 2 Laminated pattern of the wing box

	Layups	Thickness
Case 1	[0/45/-45/90/90/-45/45/0]2	2mm
Case 2	[0/45/-45/90/90/-45/45/0]6	6mm
Case 3	[0/45/-45/90/90/-45/45/0]10	10mm
Case 4	[0/45/-45/90/90/-45/45/0]14	14mm
Slenderness ratio=10		

2.4.1 Verification of Bending Analysis and Prediction Method

The results of the approximate method of the bending analysis of the composite multi-cell wing box were compared to those of the FEA to verify the accuracy. The model was set up based on the specifications of Table 1, and Cases 1–4 of Table 2 were set up based on the thickness changes. The bending analysis results are shown in Figs. 10, 11, 12, and13 for each case, respectively. Fig. 10 shows that the results are not much different from the FEM results at a thickness of 2 mm even if the compensation function is not applied. The thickness is less than 5 mm, 1/10 of 50 mm, the length of L_b, and because it is sufficiently thin, the effect of the thickness is not reflected. However, when the thickness is greater than 5 mm, as shown in Fig. 11, the error obtained using the current original method is 1.8%, and when the compensation function is used, the error is 0.8%. Next, Fig. 12 shows an error of 5% obtained using the current original method decreases to 1.5%. Similarly, in Fig. 13, the error obtained using the current original method is 10.28%, which is reduced to 2% by applying the compensation function. The thicker the thickness is, the greater the error is. However, it is confirmed that the error can be significantly reduced by applying the compensation function defined above. Table 3 shows the data values of Figs. 10, 11, 12, and 13. In the table, POM means the current original method, and PCM means the current compensation method.

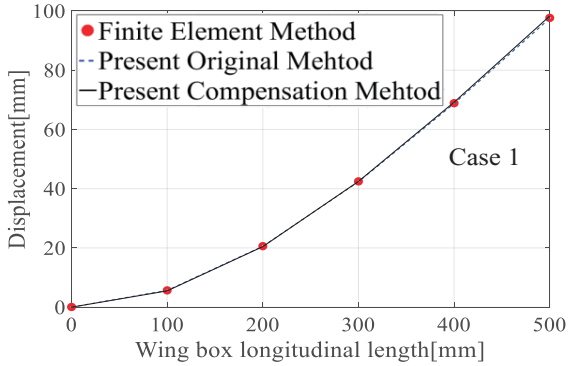

Fig. 10 Bending analysis result of composite wing box (case1)

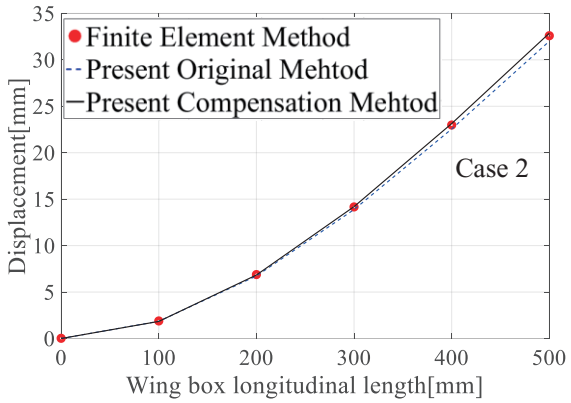

Fig. 11 Bending analysis result of composite wing box (Case2)

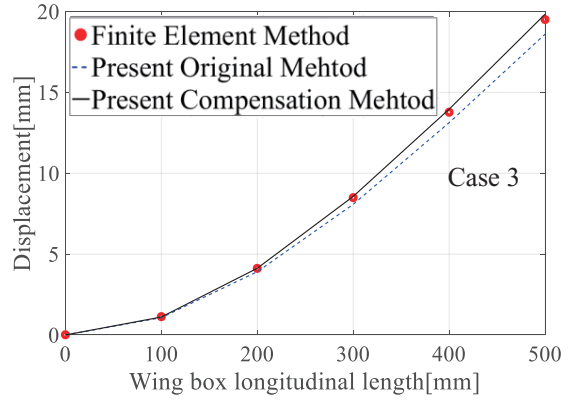

Fig. 12 Bending analysis result of composite wing box (case3)

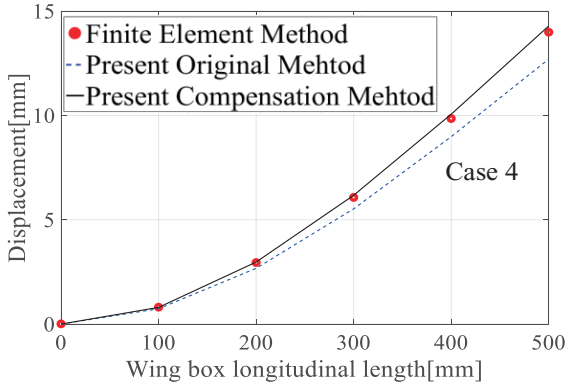

Fig. 13 Bending analysis result of composite wing box (case4)

2.4.2 Verification of Torsion Analysis and Prediction Method

The results of the approximate method of torsion analysis of the composite multi-cell wing box were compared to those of the FEA to verify accuracy. The model was set up based on the specifications of Table 1, and Cases 1, 2, 3, and4 of Table 2

Table 3 Bending analysis data of the wing box

	Thickness (mm)	Max displacement (mm)		Error (%)	
		POM	PCM	POM	PCM
Case 1	2	97.5	98.29	0.2	0.6
Case 2	6	32.0	32.86	1.8	0.8
Case 3	10	18.6	19.83	5	1.5
Case 4	14	12.7	14.28	10.3	2

were set up for the model based on the thickness changes. The torsion analysis results are shown in Figs. 14–17 for each case, respectively. compared to the results of the bending analysis, those of the torsion analysis are more sensitive to the thickness. Fig. 14 shows that results are not much different from the FEM results at a thin thickness of 2 mm even if the compensation function is not applied.

It is less than 5 mm, 1/10 of 50 mm, the length of Lb, and because it is sufficiently thin, the shear deformation and the warping effect of the thickness are not reflected. However, when the thickness is larger than 5 mm, as shown in Fig. 15, the error obtained using the current original method is 4.5%, which is reduced to 1.7% when the compensation function is applied. Next, Fig. 16 shows an error of 11.5% obtained using the current original method decreases to 2.8%. Similarly, in Fig. 17, the error obtained using the current original method is 20%, which is reduced to 4% by applying the compensation function. The thicker the thickness is, the greater the error is. However, it is confirmed that the error can be significantly reduced by applying the compensation function defined above. Table 4 shows the data values of Figs. 14, 15, 16, and17. In the table, POM means the present original method, and PCM means the present compensation method.

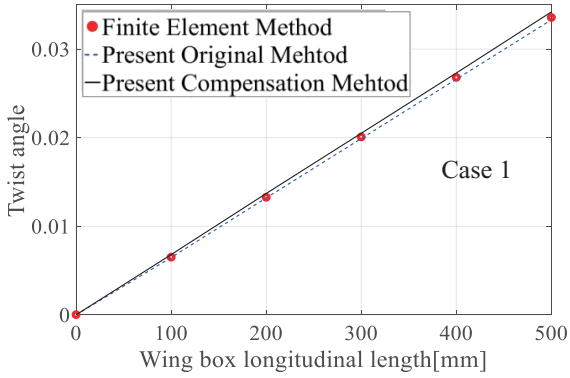

Fig. 14 Torsion analysis result of composite wing box (Case1)

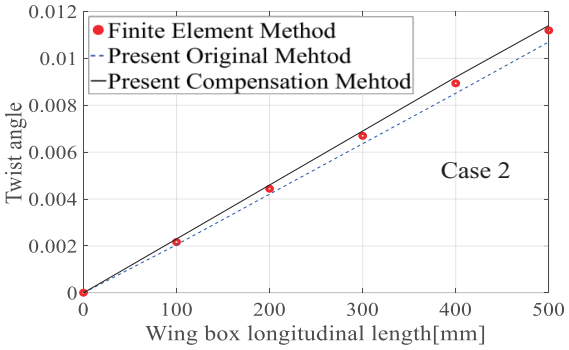

Fig. 15 Torsion analysis result of composite wing box (Case2)

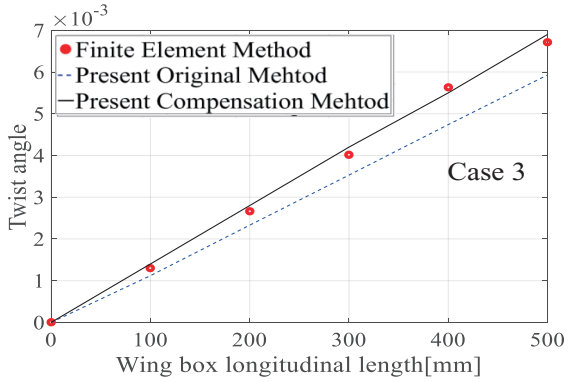

Fig. 16 Torsion analysis result of composite wing box (Case3)

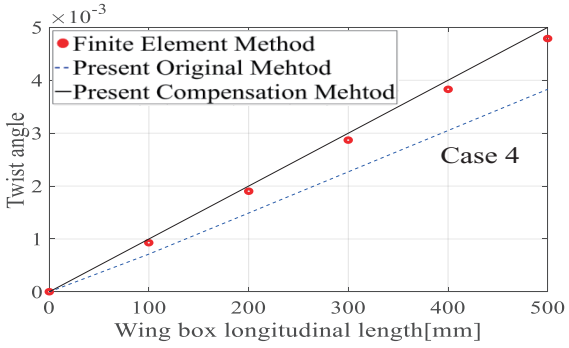

Fig. 17 Torsion analysis result of composite wing box (Case4)

2.4.3 Verification of Buckling Analysis and Prediction Method

The results of the approximate method of the buckling analysis of the composite multi-cell wing box were compared to those of the FEA to verify the accuracy. In the case of the approximate method of buckling analysis, we did not define the effective stiffness reflecting shear deformation and warping effect by the thickness increase. For the buckling of the wing box, we referred to a paper by Vincenti [6]. Vincenti conducted buckling analysis of the wing box, in which reinforcement was applied to the necessary part to focus on the buckling caused by the local buckling of the skin. In this paper, therefore, we defined and verified the approximate method of the buckling analysis while focusing on the local buckling of the skin. Fig. 18 shows the buckling analysis results of the composite wing box skin performed by the analytical method and FEM. Buckling analysis results show an error of less than 10% compared to the FEM results, and this error is caused by the mode shape according to the aspect ratio. Because the error is less than 10%, it is confirmed that the approximate method is valid. The structure optimization is performed based on the structural performance prediction methods discussed so far. The structural performance of bending, torsion, and buckling was set with constraints 1–3, and the failure index of Tasi-wu criteria was set as the fourth constraint.

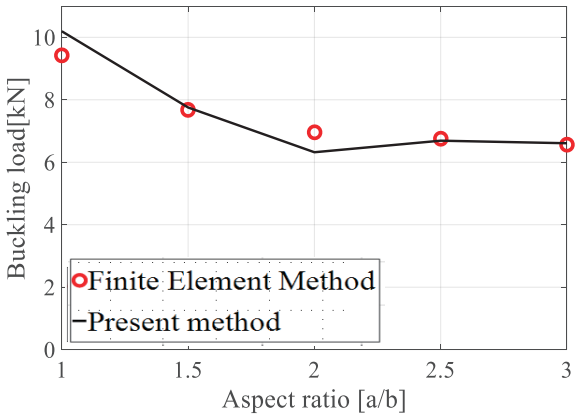

Fig. 18 Buckling analysis result of composite wing box skin

Table 4 Torsion analysis result of the wing box

	Thickness (mm)	Max Twist Angle (10^{-3})		Error (%)	
		POM	PCM	POM	PCM
Case 1	2	33.3	34.2	0.2	0.6
Case 2	6	10.7	11.4	4.5	1.7
Case 3	10	5.93	6.9	11	2.8
Case 4	14	3.83	5	20	4

2.5 Parametric Analysis of Composite Wing Box

The parametric analysis was performed to determine the validity and tendency of parameter selection. The number of spars and that of ribs was set as parameters. For the reaction, the failure index and the critical buckling load were set. Fig. 19 shows the parametric analysis result with the failure index as the reaction. When the number of spars is constant, it is confirmed that the failure index decreases as the number of ribs increases. When the number of ribs is constant, the failure index decreases as the number of spars increases.

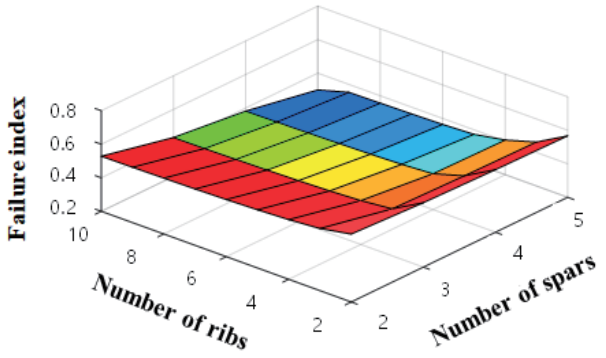

Fig. 19 Parametric analysis of a composite wing box with failure index response

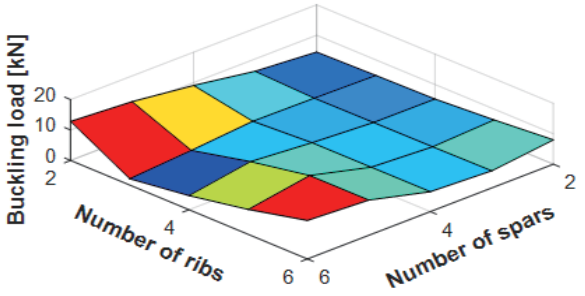

Fig. 20 Parametric Analysis of a composite wing box with buckling load response

Table 5. Wing box specifications for optimum design

Description	Value
L_a[mm]	800
L_b[mm]	400
L_c[mm]	50

Fig. 20 shows the parametric analysis results with the critical buckling load as the reaction. When the number of spars is less than four, the critical buckling load increases as the number of ribs increases. When the number of ribs is greater than three, the critical buckling load increases as the number of spars increases.

2.6 Structure Optimization of Composite Wing Box

The structure optimization was performed using a genetic algorithm, in which the generation was 100 and the population was 10. The model based on the specifications of Table 5 was used to perform the structure optimization. The results were compared by setting the single-cell wing box as the initial model, and the optimization results was verified through the FEM result. If the optimal design problem is developed, it can be represented by Eqs. (27), (28), (29), and (30).

g_1 denotes the constraint for the buckling load, g_2 for the bending displacement, g_3 for the twist angle, and g_4 for the failure index.

Min $M(n_{spar}, n_{rib}) : Mass$

Find n_{spar}, n_{rib}

S.T.

$$g_1(n_{spar}, n_{rib}) \geq 20kN \quad (27)$$

$$g_2(n_{spar}, n_{rib}) \leq 50mm \quad (28)$$

$$g_3(n_{spar}, n_{rib}) \leq 0.01° \quad (29)$$

$$g_4(n_{spar}, n_{rib}) \leq 1 \quad (30)$$

Table 6 Result of optimization

Description	Value
Number of spars [EA]	2
Number of ribs [EA]	8
Critical buckling load [kN]	24
Displacement [mm]	22.38
Twist angle	0.00658
Failure index	0.262
Mass [kg]	1.613

Table 7 Result of initial model

Description	Value
Number of spars [EA]	2
Number of ribs [EA]	2
Critical buckling load [kN]	18
Displacement [mm]	22.4
Twist angle	0.00658
Failure index	0.993
Mass [kg]	1.485

Table 8 Result of FEM

Description	Value
Number of spars [EA]	2
Number of ribs [EA]	8
Critical buckling load [kN]	25
Displacement [mm]	22.7
Twist angle	0.0066
Failure index	0.262
Mass [kg]	1.613

The structure optimization was performed based on the defined structure performance prediction method. For the required design criteria, the number of spars and ribs was set to 2 and 10, respectively, the buckling load to greater than or equal to 20 kN, the displacement to less than or equal to 50 mm, and the twist angle to less than or equal to 0.01°. Table 4 shows the results of the structure optimization performed under the required design criteria. The structure optimization results show that when the number of spars and ribs is 2 and 8, respectively, the mass is 1.613 kg, the buckling load is 24 kN, the displacement is 22.38 mm, the twist angle is 0.00658°, and the failure index is 0.262.

Furthermore, because the numbers of spars and ribs are discrete parameters, the results are also discrete. Therefore, the minimum number of discrete spars and ribs is searched within the range of satisfying the constraints, and the minimum weight is calculated accordingly. Therefore, it is confirmed that the required design criteria of the optimized composite multi-cell wing box is satisfied. Furthermore, Table 7 shows the results of setting the initial model, in which both the number of spars and ribs is two. When the number of spars is constant, it is confirmed that the increase in the number of ribs affects the failure index and the buckling load. Table 8 shows the FEM results of the structure-optimized model, and it was verified that the results are reliable compared to those of Table 6. A genetic algorithm was used for optimization, and the initial number of both spars and ribs was set to two. Furthermore, the process was performed in such a way that the optimal results were determined by searching for the lightest mass that satisfied the constraints according to the number of spars and ribs.

In this process, it is confirmed that if the structural characteristics of the wing box based on the design criteria (number of spars and ribs, material strength, etc.) does not satisfy the constraints, the results do not converge. Here, the result does not satisfy the constraints, and the number of spars and ribs is limited to a range of 2–10 to derive the minimum mass that satisfies the constraints within this range. Furthermore, because the numbers of spars and ribs are discrete values, the calculated results are also discrete. Therefore, a process was performed to search for the minimum number of discrete spars and ribs within the range that satisfies the constraints and calculate the minimum mass accordingly.

3. Conclusion

In this study, we defined the structural performance prediction equations considering the shear deformation and warping effect by the increase in the thickness of the multi-cell to perform the structure optimization of the composite multi-cell wing box. Based on this, we confirmed that the error with the structural performance prediction result is greatly reduced by introducing the compensation functions in the analytical formulas, even if the thickness of the multi-cell is increased. The contour parameters of the multi-cell wing box were defined and used to obtain the stiffness. The calculated stiffness was used to define the structural performance prediction method and apply the thickness compensation function. Then, the structural performance prediction method was validated by comparing the results to the FEA results. Furthermore, the design parameter selection and validity were verified through parametric analysis, and optimization program development and optimization of the composite multi-cell wing box was performed for lightweight. Therefore, the error was reduced by about 8% maximum in the case of bending based on the set specifications and about 16% in the case of torsion.

Through this, it is expected that a database can be built for the structural characteristics of various aircraft wings, to which composite wing boxes are applied, and it can be used when reviewing the validity of the research and analyzing the requirements of the initial design. Furthermore, it is possible to contribute to increasing the design quality by suggesting a design direction and improvement of a composite multi-cell wing box through structure optimization.

References

[1] V. V. Vasiliev, E. V. Morozov, Advanced Mechanics of composite materials and structural elements, 3rd Edition., ELSVIER 2013.

[2] E. C. Smith, “Formulation and evaluation of an analytical model for composite box-beams,” *J. Am. Helicopt*. Soc. 36, pp. 23-35, 1991.

[3] R. Chandra, I. Chopr, “Thin-walled composite beams under bending, torsional, and extensional loads,” *Journal of Aircraft*, Vol. 27, No.7, July, pp.619-626, 1990.

[4] J. M. Whitney, Structural Analysis of Laminated Anisotropic Plates, TECHNOMIC. 1987.

[5] C. T. Herakovich, Mechanics of Fibrous Composites, John Wiley & Sons, Inc. 1998.

[6] A. Vincenti, A Two- step optimisation approach for the design of composite stiffende panels partI: *global structural optimisation*, version 1 - 10 Nov 2011.

[7] C. Kim, S. R. White, “Thick-Walled Composite Beam Theory including 3-D Elastic effects and torsional warping,” *1nl. J. Solids Structures* Vol. 34, Nos 31-32, pp. 4237-4259, 1997.